

See discussions, stats, and author profiles for this publication at: <https://www.researchgate.net/publication/230752986>

# Sub-T g Cross-Linking of a Polyimide Membrane for Enhanced CO<sub>2</sub> Plasticization Resistance for Natural Gas Separation

ARTICLE *in* MACROMOLECULES · JUNE 2011

Impact Factor: 5.8 · DOI: 10.1021/ma201033j

CITATIONS

55

READS

71

6 AUTHORS, INCLUDING:



**Wulin Qiu**

Georgia Institute of Technology

49 PUBLICATIONS 1,185 CITATIONS

SEE PROFILE



**Chien-Chiang Chen**

Georgia Institute of Technology

6 PUBLICATIONS 94 CITATIONS

SEE PROFILE



**Liren Xu**

Dow Chemical Company

14 PUBLICATIONS 227 CITATIONS

SEE PROFILE



**William Koros**

Georgia Institute of Technology

252 PUBLICATIONS 8,124 CITATIONS

SEE PROFILE

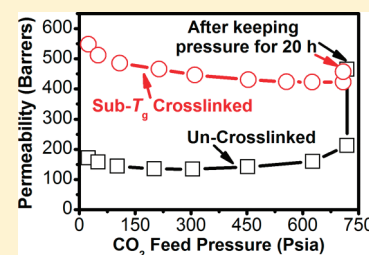
# Sub- $T_g$ Cross-Linking of a Polyimide Membrane for Enhanced $\text{CO}_2$ Plasticization Resistance for Natural Gas Separation

Wulin Qiu,<sup>†</sup> Chien-Chiang Chen,<sup>†</sup> Liren Xu,<sup>†</sup> Lili Cui,<sup>‡</sup> Donald R. Paul,<sup>‡</sup> and William J. Koros<sup>†,\*</sup>

<sup>†</sup>School of Chemical and Biomolecular Engineering, Georgia Institute of Technology, 778 Atlantic Drive, Atlanta, Georgia 30332-0100, United States

<sup>‡</sup>Department of Chemical Engineering and Texas Materials Institute, The University of Texas at Austin, Austin, Texas 78712, United States

**ABSTRACT:** Decarboxylation-induced thermal cross-linking occurs at elevated temperatures ( $\sim 15^\circ\text{C}$  above glass transition temperature) for 6FDA–DAM:DABA polyimides, which can stabilize membranes against swelling and plasticization in aggressive feed streams. Despite this advantage, such a high temperature might result in collapse of substructure and transition layers in the asymmetric structure of a hollow fibers based on such a material. In this work, the thermal cross-linking of the 6FDA–DAM:DABA at temperatures much below the glass transition temperature ( $\sim 387^\circ\text{C}$  by DSC) was demonstrated. This sub- $T_g$  cross-linking capability enables extension to asymmetric structures useful for large scale membranes. The resulting polymer membranes were characterized by swelling in known solvents for the un-cross-linked materials, TGA analysis, and permeation tests of aggressive gas feed stream at higher pressure. The annealing temperature and time clearly influence the degree of cross-linking of the membranes, and results in a slight difference in selectivity for membranes under various cross-linking conditions. Results indicate that the sub- $T_g$  thermal cross-linking of 6FDA–DAM:DABA dense film membrane can be carried out completely even at a temperature as low as  $330^\circ\text{C}$ . Permeabilities were tested for the polyimide membranes using both pure gases ( $\text{He}$ ,  $\text{O}_2$ ,  $\text{N}_2$ ,  $\text{CH}_4$ ,  $\text{CO}_2$ ) and mixed gases ( $\text{CO}_2/\text{CH}_4$ ). The selectivity of the cross-linked membrane can be maintained even under very aggressive  $\text{CO}_2$  operating conditions that are not possible without cross-linking. Moreover, the plasticization resistance was demonstrated up to 700 psia for pure  $\text{CO}_2$  gas or 1000 psia for 50%  $\text{CO}_2$  mixed gas feeds.



## INTRODUCTION

Natural gas is a cleaner burning fuel than fuel oils and coal for power plants and home heating and can also be converted to various other products such as methanol, syngas ( $\text{CO}/\text{H}_2$ ), synthetic crude oils, and diesel fuel via Fischer–Tropsch catalysis. Thus, the utilization of natural gas has become increasingly important due to the continuous increase of the worldwide demand; indeed, natural gas has become one of the fastest growing primary energy sources. Methane is the major component of natural gas, typically 50%–90% of the total; however, raw natural gas is usually contaminated with water vapor,  $\text{CO}_2$ ,  $\text{N}_2$ ,  $\text{H}_2\text{S}$ , condensable heavy hydrocarbon ( $\text{C}_3+$ ), and other gases, which must be removed with minimal loss of methane.<sup>1</sup> Of these,  $\text{CO}_2$  is the most common impurity, and it provides no heating value but causes corrosion, so it must be reduced to less than 2% to meet pipeline specifications for transport and process equipment.<sup>1–5</sup> The compositions and pressures of natural gas vary widely by geographical location, and some natural gas fields contain as much as 70%  $\text{CO}_2$  at pressures up to 5000 psia.<sup>1,3,5</sup> The processing of natural gas is the largest industrial gas separation application.<sup>1</sup> Amine absorption processes dominate the acid gas removal market, but membranes would be preferable in many cases if they are able to maintain good performance in the presence of aggressive feed streams. Normally, membrane techniques are preferred for high-concentration gas streams and amine methods are preferred for relatively low-concentration gas streams. Compared with conventional gas separation methods,

membrane techniques are particularly attractive due to the flexible design, compactness, and efficiency of the membrane units.<sup>1,5,6</sup> Obviously, there can also be significant economic advantage in building hybrid membrane/amine systems.<sup>1,7</sup>

Glassy polymeric membranes are most commonly used for high pressure natural gas separation. These polymer membranes must have good separation properties, i.e., high productivity and high selectivity, which are essential to minimize capital and operating cost. Moreover, these polymer membranes must be durable. Polyimides, especially the 6FDA-based polyimides membranes show excellent intrinsic  $\text{CO}_2/\text{CH}_4$  separation properties, thermal and chemical stabilities, and robust mechanical properties under high-pressure natural gas feeds.<sup>5,8–17</sup> In addition to high selectivity and high glass transition temperatures, 6FDA-based polyimides can be dissolved in common solvents, which allows easy fabrication of the polymer into a working device. Unfortunately, under high feed pressures,  $\text{CO}_2$  and/or other highly sorbing components tend to plasticize or swell the membranes, and thus diminish the separation efficiency of the membranes causing drastic loss in selectivity.<sup>2,5,10,12–17</sup> To develop plasticization resistance of a polymer membrane, efforts have been made through thermal treatment,<sup>18</sup> blending,<sup>19</sup> reactively formed interpenetrating networks,<sup>20</sup> and

Received: May 5, 2011

Revised: June 28, 2011

Published: July 13, 2011

cross-linking.<sup>10,12–14,17,21,22</sup> Ester cross-linking of 6FDA–DAM:DABA membranes using a diol to form ester bonds among polyimide chains have been extensively investigated in our group,<sup>5,10,13–17,23</sup> and recently, a new decarboxylation-induced thermal cross-linking was found.<sup>12</sup> Moreover, UV radiation was used to cross-link benzophenone-containing polyimide membrane,<sup>24</sup> depending on the duration of irradiation, a considerable improvement in membrane selectivity can be reached, but the permeability is strongly reduced, presumably because of the densification and reduced mobility of the polymer structure after cross-linking. Through exposure to ion beam irradiation, improved selectivity was also reached for polyimide membrane.<sup>25</sup> Polyimides can also be cross-linked with diamino compounds at ambient temperature. The imide ring was opened during cross-linking and thus polyimide backbone changed to amide structure to some extent, depending on the diamine treatment conditions.<sup>22,26–28</sup> The CO<sub>2</sub> permeability was found to be decreased after cross-linking. The thermal stability and CO<sub>2</sub>/N<sub>2</sub> selectivity of the diamine cross-linked polyimide decreased,<sup>22</sup> but H<sub>2</sub>/CO<sub>2</sub> selectivity is superior to other polymer membranes<sup>26</sup> and CO<sub>2</sub>/CH<sub>4</sub> selectivity increased largely<sup>27</sup> in cross-linked membranes. The CO<sub>2</sub> plasticization pressure was found to be increased slightly in diamine cross-linked membranes, however, the highest feed pressures tested were only about 300 psia.<sup>27,28</sup> Moreover, hydrolytic stability of such amine-opened imide backbone has not been verified as it has been for the decarboxylation induced cross-linked structures considered here. The decarboxylation-induced thermal cross-linking occurs easily at elevated temperatures (~15 °C above glass transition temperature) for 6FDA–DAM:DABA polyimide membrane, which stabilizes membrane for use in aggressive feed streams. Unfortunately, such a high temperature may result in a collapse of substructure and transition layers in asymmetric structures of a hollow fiber based on these materials. To overcome this problem, the thermal cross-linking of the 6FDA–DAM:DABA at temperatures much below its glass transition temperature (~387 °C by DSC) was developed in this work. This sub-*T<sub>g</sub>* cross-linking capability enables eventual extension to asymmetric structure useful for large scale membranes. The sub-*T<sub>g</sub>* cross-linking of polymer membranes were characterized with solubility testing, thermal analysis, and permeation tests of aggressive gas feed stream at higher pressure using both pure gases (He, O<sub>2</sub>, N<sub>2</sub>, CH<sub>4</sub>, CO<sub>2</sub>) and mixed gases CO<sub>2</sub>/CH<sub>4</sub>.

## ■ BACKGROUND AND THEORY

Permeability and selectivity are two key parameters commonly used to characterize polymeric membranes. Permeability is a measure of the membrane's intrinsic productivity, and selectivity is a measure of the separation efficiency. For dense films, the permeability ( $P_A$ ) is defined as the transmembrane partial pressure ( $\Delta p_A$ ) and thickness ( $l$ ) normalized penetrant diffusive flux ( $n_A$ ), as is shown in eq 1.

$$P_A = \frac{(n_A)l}{(\Delta p_A)} \quad (1)$$

Under high pressure, it is more appropriate to describe the permeation driving force in terms of a fugacity difference rather than a partial pressure difference, i.e., the fugacity difference of component  $i$  between the upstream and downstream, due to the nonideal gas behavior for natural gas mixtures. For dense films, permeability ( $P_A$ ) is defined as the flux ( $n_A$ ), normalized by the

transmembrane fugacity driving force of component A ( $\Delta f_A$ ) and membrane thickness ( $l$ ), as described in eq 2.

$$P_A = \frac{(n_A)l}{(\Delta f_A)} \quad (2)$$

Equation 2 was used to calculate the gases permeabilities. The fugacity coefficients of condensable CO<sub>2</sub> and CH<sub>4</sub> were calculated from the virial equation of state<sup>29</sup> using the pure-component second virial coefficients<sup>30</sup> and the second virial coefficient for the binary mixture.<sup>29</sup>

The unit for permeability is “barrer”, which has the following meaning: 1 barrer =  $10^{-10} \text{ cm}^3 (\text{STP}) \cdot \text{cm} / (\text{s} \cdot \text{cm}^2 \cdot \text{cmHg})$ . Another popular unit for permeability is  $(\text{kmol} \cdot \text{m}) / (\text{m}^2 \cdot \text{s} \cdot \text{kPa})$ , which can be converted to barrer by multiplication by  $2.99 \times 10^{15}$ .

The ideal selectivity (i.e., pure gas feed) between two gases A and B is defined as the ratio of their permeabilities (or permeances for asymmetric hollow fiber membranes), is given in eq 3.

$$\alpha_{AB} = \frac{P_A}{P_B} \quad (3)$$

Permeation occurs through polymer membranes via a coupled diffusion and sorption mechanism, so the permeability equals the product of the effective diffusion coefficient,  $D$ , and sorption coefficient,  $S$ , of a component A in a given membrane, as shown in eq 4.

$$P_A = D_A S_A \quad (4)$$

For mixed-gas feeds, the “separation factor” is a practical measure of the separation efficiency, however, compared with selectivity, is less useful in describing intrinsic behavior of a membrane material unless the downstream pressure is very low, which it is in this study. The separation factor is calculated by eq 5.

$$\alpha_{AB} = \frac{(y_A/y_B)}{(x_A/x_B)} \quad (5)$$

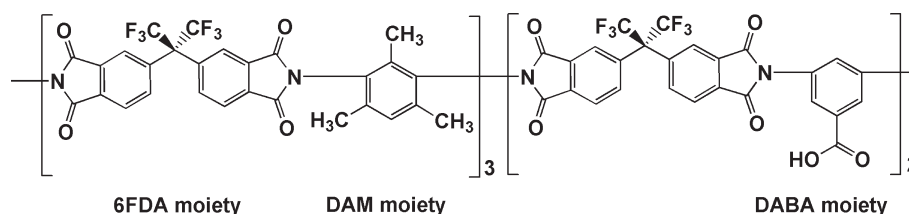
where  $x_i$  is the mole fraction of component  $i$  on the feed side and  $y_i$  the mole fraction of component  $i$  on the permeate side, as measured by gas chromatography (GC).

## ■ EXPERIMENTAL SECTION

**Materials.** (4,4'-Hexafluoroisopropylidene) diphthalic anhydride (6FDA), 2,4,6-trimethyl-1,3-diaminobenzene (DAM), and 3,5-diaminobenzoic acid (DABA) were purchased from Aldrich. Monomers were purified through sublimation or recrystallization, and were stored separately under high vacuum before synthesis. 1-methyl-2-pyrrolidinone (NMP), Acetic anhydride (Ac<sub>2</sub>O), and 1,3-propanediol were dried with molecular sieves before use.

**Polymer Synthesis.** The polyimide, 6FDA–DAM:DABA (3:2) was synthesized through the condensation of the dianhydride with diamine, its chemical structure is shown in Scheme 1, and the mole ratio of DAM to DABA is 3 to 2. The synthesis is a two-step reaction in which the first step produces a high molecular weight polyamic acid (PAA) at low temperature (~5 °C), and a second step is to imidize, i.e., to close the ring by releasing water and producing chemical stable polyimide (PI). In the first step, stoichiometric amount of the monomers were dissolved in NMP to make a 20 wt % solution, and stirred under N<sub>2</sub> purge for 24 h to produce PAA solution. Chemical imidization was carried out in the second step. The PAA solution was stirred in the presence of beta picoline and acetic anhydride at ambient temperature for 24 h under N<sub>2</sub> purge. The resulting polyimide were precipitated and washed with methanol, dried at 210 °C under vacuum for 24 h. The

Scheme 1. Chemical Structure of 6FDA–DAM:DABA(3:2) Polyimide



FTIR and TGA results of the resulting polyimide show a complete imidization.

**Membrane Formation.** The dense film membrane was cast on a Teflon-covered glass plate from a THF solution inside a controlled environment glovebag to promote slow evaporation of the solvent. A casting knife with a 12 mil clearance was used to draw the solution into a film of uniform thickness. After completion of the evaporation of THF solvent, the membrane was removed from the plate, and dried at 180 °C for 24 h under vacuum.

The obtained membranes were thermally treated at given temperatures below their glass transition temperature using a controlled procedure and environment. A Thermcraft split-tube furnace was outfitted with an internal thermocouple for temperature control, and an argon purge was maintained at 200 mL/min during the process. Membranes were put on a smooth aluminum sheet over a stainless steel support, and argon was purged until the system reached steady state prior to thermal treatment. The thermal treatment procedure comprises heating from 300 at 10 K/min to a temperature, which is 50 K below the desired temperature, followed by heating at 1 K/min to the desired temperature, and dwelling at the temperature for a given period of time. Finally, membranes were removed from the furnace and quenched rapidly to room temperature in air.

**Characterization.** Molecular weights of the polymers were determined by GPC using a Waters 2410 Separations Module equipped with Styragel HR 4, 3, and 1 columns. The detection was performed by a Waters 410 Refractive Index Detector. Samples were dissolved in THF at 1 wt % concentration.

Fourier transform infrared (FTIR) spectra were recorded by a Bruker Tensr 27 spectrophotometer at a resolution of 2 cm<sup>-1</sup> with the coaddition of 300 scans in the spectral range of 4000–400 cm<sup>-1</sup>.

Thermogravimetric analysis (TGA) and derivative weight data were recorded on a TA Q-5000 analyzer at a heating rate of 10 K/min under a nitrogen atmosphere, using ~10 mg sample.

Differential scanning calorimetry (DSC) was carried on a TA Q-200 at a heating (or cooling) rate of 10 K/min in nitrogen atmosphere. The sample was heated to 400 °C and isothermal for 1 min, cooled to and equilibrated at 50 °C, and reheated to 400 °C. The glass transition temperature was taken from the second heating run.

TGA-MS was performed in a TA Instruments Q500 thermal gravimetric analysis (TGA) instrument coupled to a Pfeiffer ThermoStar mass spectrometer (MS) under nitrogen atmosphere at a heating rate of 10 K/min.

Wide-angle X-ray diffraction (WAXD) was measured on a PAnalytical X'pert Pro diffractometer operating with a Cu K $\alpha$  radiation at a wavelength of 1.54 Å, in a 2 $\theta$  range of 5–45°.

The polymer solubility was determined visually by immersing a polymer film in NMP for a given temperature and time.

The dried and thermally treated membranes were used for gas permeation tests. The membrane was masked using impermeable aluminum tape to define the permeable area, and epoxy was applied at the interface of the tape and the open area of the membrane to ensure against bypassing the membrane. The masked membranes were loaded into a permeation cell and assembled to a permeation system. Both

upstream and downstream of the permeation system were evacuated thoroughly for about 3 days, at roughly 0.01 Torr. The range of the downstream transducer is 10 Torr, and the measurements of steady-state gas permeabilities were performed at 35 °C with a constant volume, variable pressure apparatus described earlier.<sup>10</sup> The pressure rise ( $dp/dt$ ) in a standard downstream volume was monitored with time by LabView through an accurate pressure transducer, and was calculated from data in the range 8–10 Torr. The measured leak rates were 10<sup>-7</sup> to 10<sup>-6</sup> Torr/min in the downstream receiving volume. This leak comprises less than 1% of the pressure rise rate seen even for the lowest feed pressure of the lowest permeability gas (CH<sub>4</sub>). For mixed gas measurements, the permeate gas sample in the downstream receiver was analyzed by gas chromatography (GC). The measurements were repeated 2–3 times for a pure gas measurements, and 4–5 time for a mixed gas measurements, at a given feed pressure. Replicates (at least two and generally three separate samples of each membrane preparation) were made and found to differ by less than 10% for permeability, with essentially no difference for selectivity.

## RESULTS AND DISCUSSION

The introduction of the  $-C(CF_3)_2-$  linkage restricts the torsional motion of neighboring phenyl rings and tends to enhance the permselectivity for CO<sub>2</sub> over CH<sub>4</sub>.<sup>9,11,31,32</sup> In 6FDA–DAM:DABA copolyimides, the introduction of DAM backbone provides high gas permeability for the membrane, while the DABA backbone provides reactive acid sites that are useful for cross-linking and/or modification. To impose plasticization resistance of aggressive gas feed streams for the polymer membranes, ester cross-linking of membranes was investigated and found to proceed in two steps: (1) produce a monoester “cross-linkable” polyimide through reacting of 6FDA–DAM:DABA polymer with various diols during the polymer synthesis process, where the resulting cross-linkable polyimide can be processed in a solution into a membrane form, and (2) gain ester bond cross-linked polymer membrane through transesterification/cross-linking reaction in the solid state of the formed membrane at elevated temperatures.<sup>5,10,13,17,23</sup> More recently, decarboxylation-induced thermal cross-linking at 389 °C (15 °C above  $T_g$ ) was found for 6FDA–DAM:DABA (2:1).<sup>12</sup> Herein, we are interested in thermal cross-linking below the polymer's glass transition temperature since this will avoid any partial pyrolysis of the polymer and alleviate the negative impact on the skin and porous substructure of a hollow fiber membrane.

**Sub- $T_g$  Cross-Linking Due to Decarboxylation of the DABA Moiety.** The molecular weight of the polyimide 6FDA–DAM:DABA (3:2) as measured by GPC was found to be 278,000 ( $M_w$ ) with a polydispersity of 3.5. The glass transition temperature was determined by DSC to be 387 °C, defined as the inflection point of the change in the heat capacity during a second heating. Figure 1 shows the typical FTIR and TGA curves of the



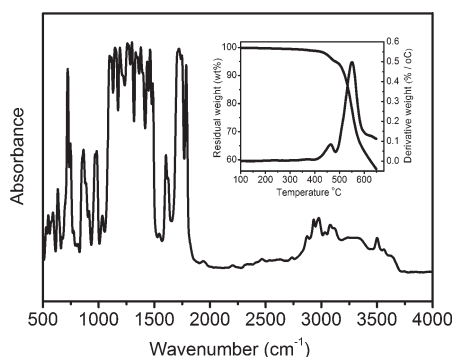


**Figure 1.** Typical FTIR and TGA curves of 6FDA-DAM:DABA (3:2) polymer.

6FDA-DAM:DABA (3:2) polymer. The characteristic peaks of polyimide are seen at  $1785\text{ cm}^{-1}$  (symmetric C=O stretching vibration),  $1725\text{ cm}^{-1}$  (asymmetric C=O stretching vibration), and  $720\text{ cm}^{-1}$  (deformation of imide ring band of OC-N-CO); no characteristic peaks of amide groups at  $1650$  and  $1550\text{ cm}^{-1}$ , from C=O and N-H bending of an amide group, respectively, are seen, indicating that the polyamic acid was imidized completely. The broad weak absorption at  $3200\text{--}3500\text{ cm}^{-1}$  is attributed to the vibration band of -OH in DABA moiety.<sup>33</sup> The carbonyl stretching of the acid group was partially overlapped with the absorption of the imide carbonyl. In the TGA trace of 6FDA-DAM:DABA (3:2) polymers, no weight loss was found until  $400\text{ }^{\circ}\text{C}$ , indicating that all polyamic acid was completed converted to polyimide, in agreement with the FTIR results. Prior to major backbone degradation starting at about  $500\text{ }^{\circ}\text{C}$ , a minor weight loss starting at about  $400\text{ }^{\circ}\text{C}$ , accordingly, a smaller peak at  $465\text{ }^{\circ}\text{C}$  is observed prior to the large peak at  $550\text{ }^{\circ}\text{C}$  in the derivative weight curve. The first minor degradation was attributed to the removal of carboxylic groups in DABA moieties. Similar thermal behavior was observed for other polyimides containing carboxylic pendant groups.<sup>12,33-36</sup> This conclusion is supported further by results of polymer without carboxylic acid groups, i.e., 6FDA-DAM, as shown in Figure 2. The intensities of atomic masses,  $m/z = 44$ , attributed to  $\text{CO}_2$ , and  $m/z = 69$ ,  $-\text{CF}_3$  fragments shown in Figure 2 are in relation to temperature. In addition to the major peak at high temperature, compared with the 6FDA-DAM polymer, the 6FDA-DAM:DABA (3:2) polymer shows also a small peak at lower temperature in the derivative weight curve in Figure 2a. Only one peak of  $\text{CO}_2$  fragments was found at about  $530\text{ }^{\circ}\text{C}$ , which was caused by the degradation of the polymer backbone for 6FDA-DAM in Figure 2b; however, 6FDA-DAM:DABA(3:2) polymer showed two  $\text{CO}_2$  peaks. In Figure 2c, the  $-\text{CF}_3$  peak was found at  $495\text{ }^{\circ}\text{C}$  for 6FDA-DAM polymer and  $480\text{ }^{\circ}\text{C}$  for 6FDA-DAM:DABA (3:2) polymer. Obviously, the  $\text{CO}_2$  peak at lower temperature in Figure 2b was caused mainly by the degradation of carboxylic acid groups in DABA moieties. The emergence of  $\text{CO}_2$  from carboxylic acid groups starts at about  $330\text{ }^{\circ}\text{C}$  and is finished at about  $460\text{ }^{\circ}\text{C}$ , followed by the emergence of  $\text{CO}_2$  from main backbone degradation of 6FDA-DAM:DABA (3:2) polymer.

The minor weight loss in the TGA curve as well as the corresponding smaller peak in the derivative weight curve at lower temperature is characteristic of decarboxylation of -COOH moieties, which is useful for characterizing the decarboxylation-induced cross-linking of the polymer. It was found that cross-linking occurred for 6FDA-DAM:DABA (2:1) at

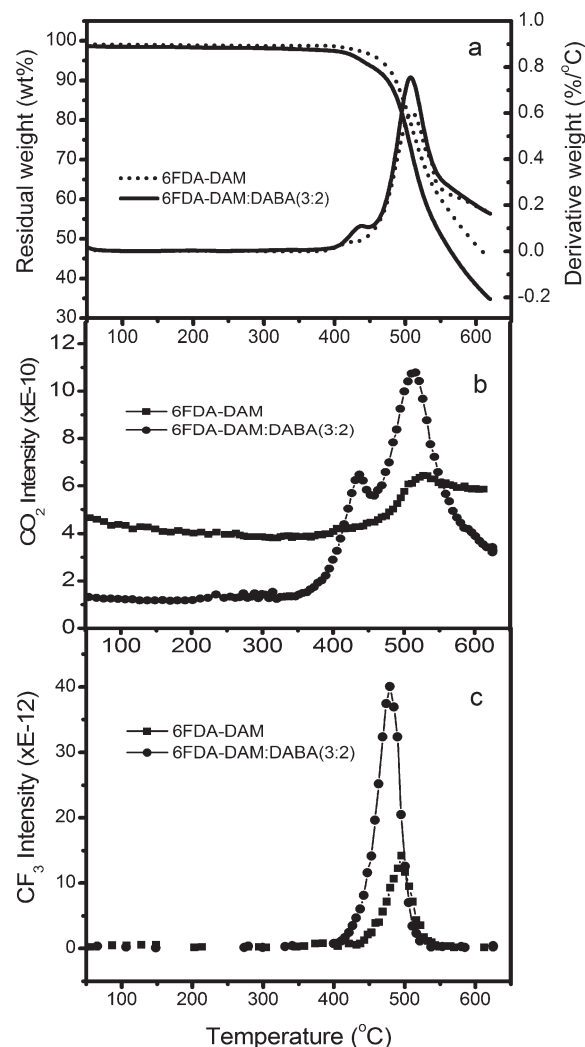


**Figure 2.** Results of (a) TGA, and MS of evolving gases of (b)  $\text{CO}_2$ , and (c)  $\text{CF}_3$  of 6FDA/DAM and 6FDA-DAM:DABA(3:2) polymers during TG analysis.

elevated annealing temperatures of about  $15\text{ }^{\circ}\text{C}$  above  $T_g$ , when the pendant acid group decarboxylated to create a phenyl radical capable of attacking other portions of the polyimide for cross-linking.<sup>12</sup> To avoid the collapse of the substructure of a hollow fiber membrane, which may result in a loss of permeance and possible loss in selectivity, a modified protocol was used. Specifically, a low thermal treatment temperature annealing below the polymer's  $T_g$  (herein,  $387\text{ }^{\circ}\text{C}$ ) was carried out to investigate the feasibility of decarboxylating the pendant -COOH group to enable cross-linking as decarboxylation.

As described above, the decarboxylation of -COOH group can be monitored by the minor weight loss at low temperatures in TGA curves (i.e., the smaller peak in derivative weight curve). As seen in Figure 3, the membranes that were thermally treated below  $330\text{ }^{\circ}\text{C}$  yielded similar curves as those shown in Figure 1; however, the smaller peak at low temperatures associated with decarboxylation varies with the specific sample prethermal history. As shown in Figure 3a, after annealing at  $120\text{ }^{\circ}\text{C}$  in Ar for 24 h, trace solvent was possibly still left in membrane, since a slow weight loss was observed at around  $190\text{ }^{\circ}\text{C}$ . When the membrane was annealed at  $180$  or  $220\text{ }^{\circ}\text{C}$ , the slow weight loss

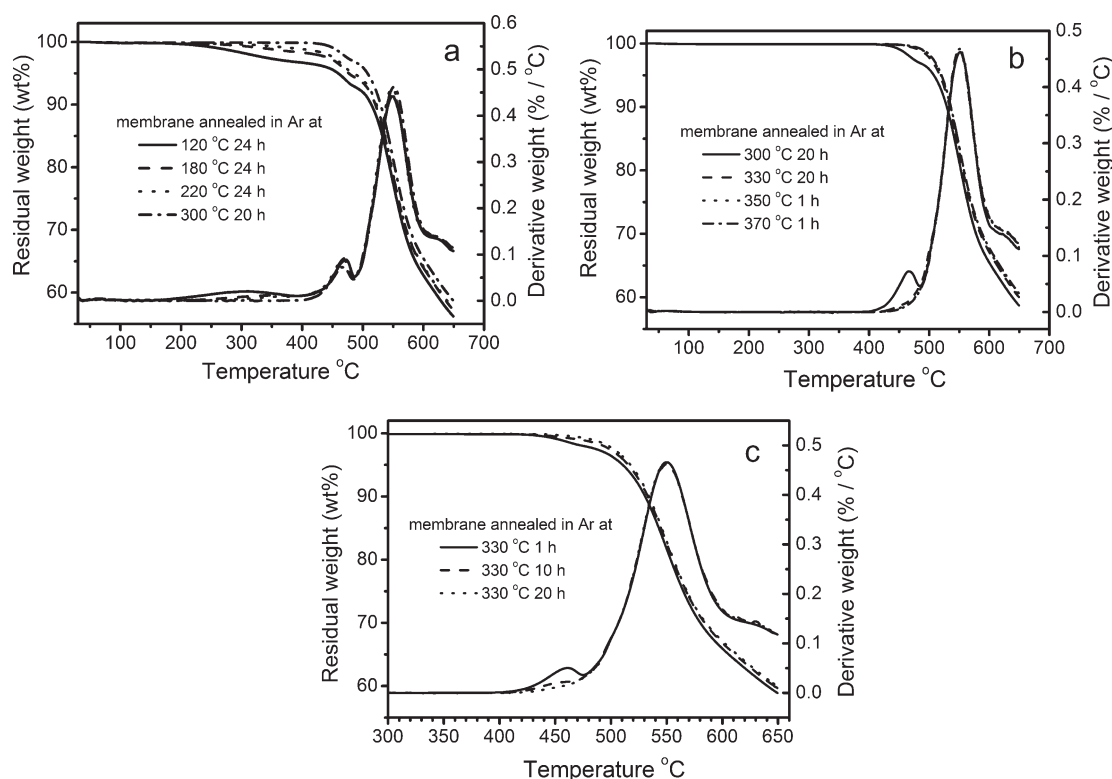


Figure 3. TGA curves of the polyimide thermally treated under different conditions.

started at about 290 °C. In addition to the decarboxylation peak at 460–470 °C, the positive derivations at about 300 °C might result from the trace solvents. When the membrane was annealed at 300 °C for 20 h, both the slow weight loss and the lower temperature derivative peak were barely observed, indicating all solvent was evaporated. The weight loss and the smaller peak due to decarboxylation get smaller, indicating that the decarboxylation of pendant carboxylic acid groups initiates at about 300 °C. Figure 3b shows that the pendant  $\text{—COOH}$  groups can be removed almost completely from the polyimide membranes within 1 h by annealing either at 370 °C or at 350 °C, or at 330 °C for 20 h. In these curves, only the large weight loss at higher temperatures, i.e., the large peak at high temperatures in the derivative weight curves, was seen; the decarboxylation-caused weight loss disappeared. TGA results for the membrane annealed at 330 °C for 20 h is almost the same as that at 350 °C for 1 h, although not identical. The TGA results for the membrane annealed at 370 °C for 1 h is identical to that of at 370 °C for 5 h (not shown in Figures), indicating that 1 h is enough to remove all  $\text{—COOH}$  groups from the membrane at 370 °C. Figure 3c shows that when the membrane was annealed at 330 °C for 20 h almost all of the  $\text{—COOH}$  groups in DABA moieties were removed. These results are consistent with those from FTIR spectroscopy, as can be seen in Figure 4; the broad weak absorption at 3200–3500  $\text{cm}^{-1}$ , attributed to  $\text{—OH}$  vibration of carboxylic acid group in DABA moiety<sup>33</sup> gets weaker with increasing of thermal treatment temperature and finally disappeared in the membranes annealed at 330 °C for 20 h or at 370 °C for 1 h.

The membranes thermally treated under the conditions in Figure 3 were tested for their solubility. Membranes thermally treated below 300 °C were dissolved easily in NMP at room temperature. Membranes thermally treated at 300 °C for 20 h or

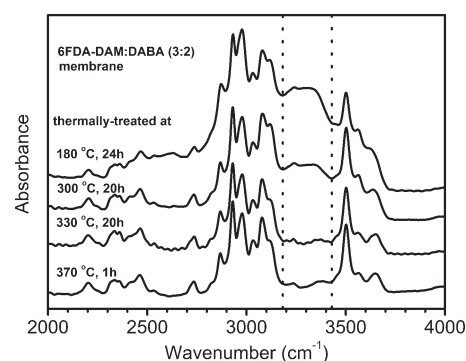
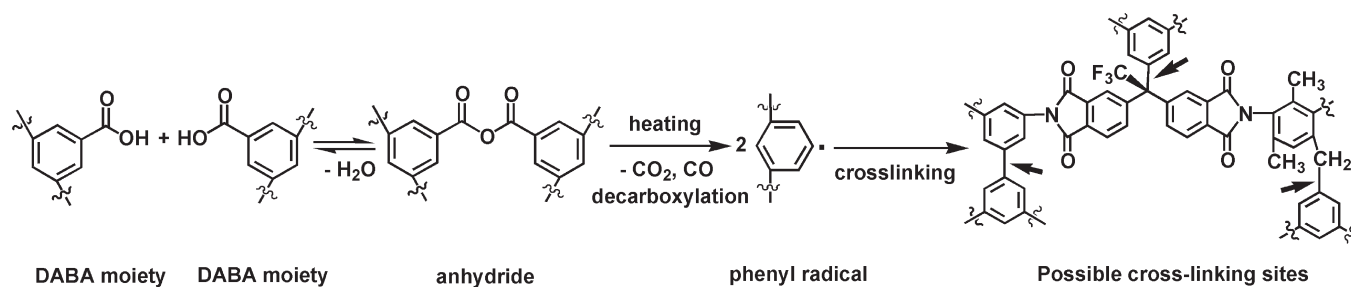


Figure 4. FTIR spectroscopy of the polyimide thermally treated under different conditions.

330 °C for 1 h swelled at room temperature and left very small amount of gels in hot NMP at 100 °C; i.e., they partially dissolved, indicating that these membranes were only partially cross-linked and the cross-linked fractions were very low. Membranes thermally treated at 330 °C for 10 h swelled in hot NMP with very small amount dissolved. Membranes thermally treated at 350 or 370 °C for 1 h, or at 330 °C for 20 h were insoluble even in hot NMP at 100 °C for 1 week, indicating the membranes were highly cross-linked. The above results indicate that decarboxylation-induced cross-linking of 6FDA–DAM:DABA (3:2) membrane can be performed at a temperature much below its  $T_g$  (387 °C). The proposed mechanism of this decarboxylation-induced thermal cross-linking is illustrated in Scheme 2, where the possible cross-linking bonds noted earlier<sup>12</sup> are noted with an arrow. The decarboxylation, radical-induced cross-linking occurs via a dianhydride intermediate. Two  $\text{—COOH}$  groups in

Scheme 2. Decarboxylation-Induced Cross-Linking Mechanism and Possible Cross-Linking Sites of DABA-Based Polyimide



adjacent DABA moieties form an anhydride during heating under vacuum or inert gas flow. The anhydride is subsequently decarboxylated by release of a  $\text{CO}_2$  and a  $\text{CO}$ , thereby creating two phenyl free radicals at sufficiently high temperature. Most likely the resulting neighboring phenyl radicals combine to form linkages that yield biphenyl cross-linking; the resulting phenyl radical might also abstract a hydrogen from methyl groups in DAM moieties to create a methyl radical and a cross-linking site; at higher temperature, the  $-\text{CF}_3$  groups may also be cleaved and provide an available radical site for cross-linking. Nevertheless, all three potential sites illustrated in Scheme 2 are viable stabilizing linkages. While free radical decomposition of the anhydride may begin above  $220^\circ\text{C}$ , more efficient decarboxylation and actual biphenyl cross-links involving additional nanoscale rearrangements seems to require higher temperatures, but still below  $T_g$ . In fact, the additional two sites in Scheme 2 are only mentioned for completeness, and are not believed to be as important as the first primary site leading to the biphenyl linkage. In any case, large-scale backbone decomposition does not begin to occur until much higher temperatures, near  $450$ – $470^\circ\text{C}$  as indicated by small amount of  $\text{HCF}_3$  evolution in TGA-IR analysis in Figure 2. This indicates that the basic polymer nature is preserved in such decarboxylation, radical-induced cross-linked materials.

**Effects of Cross-Linking on Average Interchain Distance (*d*-Spacing).** Figure 5 shows the wide-angle X-ray scattering patterns of some typical membranes, it is observed that all the membranes are in an amorphous state without any crystalline phase. Compared with the membrane annealed at  $180^\circ\text{C}$ , the  $2\theta$  value of  $120^\circ\text{C}$  dried membrane shifted to right, i.e., the larger diffraction angle, while the  $2\theta$  values of membranes thermally treated at higher temperature shifted to the left. The average interchain distances (*d*-spacing) values were calculated by Bragg's law ( $d = \lambda/2(\sin \theta)$ ) using the maximum  $2\theta$  values of the broad peaks. Although *d*-spacing cannot be used as a true interchain distance, the changes of *d*-spacing can be taken as an indicator of the amount of room available for penetrating small molecules to diffuse through these membranes.<sup>37</sup> The membrane dried at  $120^\circ\text{C}$  had a *d*-spacing of  $5.86\text{ \AA}$ . As expected, after annealing and removal of trace solvent at  $180^\circ\text{C}$ , the membrane showed a decreased *d*-spacing of  $5.63\text{ \AA}$ , indicating an increasing chain packing density. Thermal treatment of the membrane at or above  $330^\circ\text{C}$  shown an increased *d*-spacing of  $6.18\text{ \AA}$  ( $330^\circ\text{C}$ ),  $6.43\text{ \AA}$  ( $350^\circ\text{C}$ ), and  $6.55\text{ \AA}$  ( $370^\circ\text{C}$ ) and indicates that the average interchain distance increases due to the decarboxylation-induced cross-linking. In contrast to annealing and physical aging which reduce free volume,<sup>38,39</sup> the results imply that the free volume within the membrane (the amount of space available for penetrating small molecules through membranes) increased as a result of cross-linking.

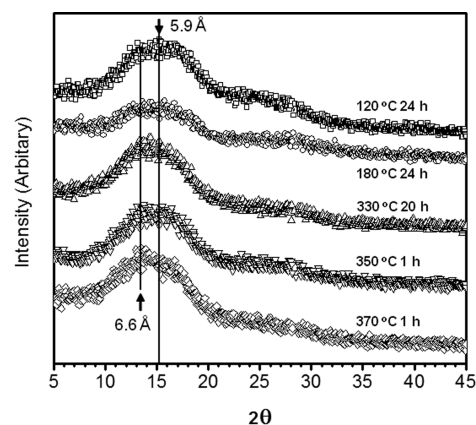


Figure 5. WAXD patterns of membranes thermally treated under different conditions.

Table 1. Permeabilities from Pure Gases for Polyimide Membranes at 100 psia and  $35^\circ\text{C}$  (barrer)

| thermal-treatment conditions            | He    | $\text{O}_2$ | $\text{N}_2$ | $\text{CH}_4$ | $\text{CO}_2$ |
|---|-------|--------------|--------------|---------------|---------------|
| $120^\circ\text{C}$ , 24 h              | 203.9 | 33.5         | 7.5          | 4.7           | 161.1         |
| $180^\circ\text{C}$ , 24 h              | 195.9 | 32.0         | 7.0          | 4.2           | 144.0         |
| $300^\circ\text{C}$ , 20 h              | 257.0 | 44.5         | 10.0         | 6.0           | 202.9         |
| $330^\circ\text{C}$ , 1 h               | 276.3 | 63.4         | 15.4         | 10.4          | 290.0         |
| $330^\circ\text{C}$ , 10 h              | 317.0 | 66.5         | 15.8         | 10.2          | 289.6         |
| $330^\circ\text{C}$ , 20 h <sup>a</sup> | 333.3 | 79.0         | 19.3         | 12.9          | 350.1         |
| $350^\circ\text{C}$ , 1 h <sup>a</sup>  | 286.4 | 69.3         | 15.4         | 11.8          | 340.8         |
| $370^\circ\text{C}$ , 1 h <sup>a</sup>  | 357.0 | 98.0         | 25.2         | 18.1          | 485.4         |

<sup>a</sup> Membranes were highly cross-linked.

**Effects of Cross-Linking on Pure Gases Permeation Properties.** The gas permeabilities were tested in the sequence He,  $\text{O}_2$ ,  $\text{N}_2$ ,  $\text{CH}_4$ , and  $\text{CO}_2$ . The purity of the He was 99.9999%, which this for the other gas was 99.999%. Membrane was exposed to the feed stream for 2–3 h to allow sufficient equilibration time to reach steady state before permeation measurements. Then permeation measurement was made, and to double check the achievement of steady state, this was followed by evacuating the downstream, while the upstream was kept exposed in feed pressure for another 2–3 h to allow any slow relaxations involved in plasticization, before the second measurement was made. The measurement was repeated 2–3 times, and the standard derivation was found less than 0.5% for all gases. Table 1 summarizes the permeabilities of the pure gases measured at 100 psia, and the ideal selectivities from eq 3 are listed in Table 2.

**Table 2.** Selectivities from Pure Gases for Polyimide Membranes at 100 psia and 35 °C

| thermal-treatment conditions | He/CH <sub>4</sub> | He/N <sub>2</sub> | O <sub>2</sub> /CH <sub>4</sub> | O <sub>2</sub> /N <sub>2</sub> | CO <sub>2</sub> /CH <sub>4</sub> | CO <sub>2</sub> /N <sub>2</sub> | N <sub>2</sub> /CH <sub>4</sub> |
|------------------------------|--------------------|-------------------|---------------------------------|--------------------------------|----------------------------------|---------------------------------|---------------------------------|
| 120 °C, 24 h                 | 43.1               | 27.1              | 7.1                             | 4.5                            | 34.0                             | 21.4                            | 1.6                             |
| 180 °C, 24 h                 | 46.8               | 27.8              | 7.6                             | 4.6                            | 34.4                             | 20.4                            | 1.7                             |
| 300 °C, 20 h                 | 43.1               | 25.7              | 7.5                             | 4.5                            | 34.0                             | 20.3                            | 1.7                             |
| 330 °C, 1 h                  | 26.5               | 17.9              | 6.1                             | 4.1                            | 27.8                             | 18.8                            | 1.5                             |
| 330 °C, 10 h                 | 31.2               | 20.1              | 6.5                             | 4.2                            | 28.4                             | 18.4                            | 1.5                             |
| 330 °C, 20 h <sup>a</sup>    | 25.8               | 17.3              | 6.1                             | 4.1                            | 27.1                             | 18.2                            | 1.5                             |
| 350 °C, 1 h <sup>a</sup>     | 24.2               | 16.3              | 5.9                             | 4.0                            | 28.8                             | 19.4                            | 1.5                             |
| 370 °C, 1 h <sup>a</sup>     | 19.7               | 14.3              | 5.4                             | 3.9                            | 26.8                             | 19.3                            | 1.4                             |

<sup>a</sup> Membranes were highly cross-linked.

The above thermal treatments at temperature below 300 °C caused no cross-linking, and the permeability of the membranes are influenced by physical annealing effects. It is expected that annealing can form charge transfer complexes (CTCs),<sup>12</sup> and enhance hydrogen bonds among –COOH groups, thereby “tightening” the polymer segmental packing and reducing the free volume within the polymer matrix. The changes induced such annealing is a reduction in gas permeability. The TGA results show that membrane annealed at 120 °C retained trace amounts of solvents. Annealing at higher temperatures eliminates residual solvent. As can be seen in Table 1, when the annealing temperature increased from 120 to 180 °C, the permeability of all gas decreases, in the order of CH<sub>4</sub> (11.6%) > CO<sub>2</sub> (10.6%) > N<sub>2</sub> (6.7%) > O<sub>2</sub> (4.5%) > He (3.9%). The permeability of the condensable gases (CO<sub>2</sub> and CH<sub>4</sub>) decreases more than the permeability of the less condensable gases (He, O<sub>2</sub>, and N<sub>2</sub>). The penetrant condensability is reflected by its critical temperature, and have the order of CO<sub>2</sub> (304.2 K) > CH<sub>4</sub> (190.7 K) > O<sub>2</sub> (154.4 K) > N<sub>2</sub> (126.1 K) > He (5.2 K). Except for CO<sub>2</sub>, the permeability decreases in the same order as the kinetic diameter of penetrant gases, i.e., CH<sub>4</sub> (3.8 Å) > N<sub>2</sub> (3.64 Å) > O<sub>2</sub> (3.46 Å) > CO<sub>2</sub> (3.3 Å) > He (2.6 Å). The larger permeability drop of CO<sub>2</sub> versus N<sub>2</sub> and O<sub>2</sub> might reflect the elimination of excess free volume sites that are favorable to accommodate the more condensable penetrants. Therefore, with the reduction of free volume caused by annealing, the permeability of the condensable gases drops more than for the less condensable gases. As expected, Table 2 shows a larger increase for membranes annealed at 180 °C than those annealed at 120 °C for all the gas pairs except CO<sub>2</sub>/N<sub>2</sub>. The decrease in CO<sub>2</sub>/N<sub>2</sub> selectivity may result from the greater reduction in permeability of CO<sub>2</sub> versus N<sub>2</sub>, due to the loss in excess free volume noted in the earlier discussion of annealing.

Because the membrane annealed at 120 °C contains trace amounts of solvent, the membrane annealed at 180 °C is used as the standard to compare with other membranes treatments. For the 300 °C treated membrane, which may be partially cross-linked, an increase in permeabilities is observed in Table 1; however, selectivities changed very little as shown in Table 2, compared with the membrane annealed at 180 °C. When the membranes were annealed at 330 °C, a marked jump in permeability for all gases is observed. Compared with the membranes annealed at 180 °C, the membrane annealed at 330 °C for even just 1 h shows a jump in permeability as 148% (CH<sub>4</sub>), 120% (N<sub>2</sub>), 101% (CO<sub>2</sub>), 98% (O<sub>2</sub>), and 41% (He), respectively. The selectivity of all gas pairs decreased, in the order of He/CH<sub>4</sub> (43%) > He/N<sub>2</sub> (36%) > O<sub>2</sub>/CH<sub>4</sub> (20) > CO<sub>2</sub>/CH<sub>4</sub> (19%) > N<sub>2</sub>/CH<sub>4</sub> (12%) > O<sub>2</sub>/N<sub>2</sub> (11%) > CO<sub>2</sub>/N<sub>2</sub> (8%).

The membrane gained high cross-linking density after being thermally treated at 330 °C for 20 h, or at 350 or 370 °C for 1 h, as discussed earlier. Within the experimental conditions, the permeability increases due to increased thermal treatment temperature, reflecting the more open matrix after cross-linking. It can be observed that the permeabilities of the membrane annealed at 370 °C were significantly higher than the other samples. Specifically, compared with membranes annealed at 180 °C, the permeability of membrane annealed at 370 °C for 1 h, increased about 332% (CH<sub>4</sub>), 260% (N<sub>2</sub>), 237% (CO<sub>2</sub>), 206% (O<sub>2</sub>), and 82% (He), respectively. The selectivity decreased in the order of He/CH<sub>4</sub> (58%) > He/N<sub>2</sub> (49%) > O<sub>2</sub>/CH<sub>4</sub> (29%) > CO<sub>2</sub>/CH<sub>4</sub> (22%) > N<sub>2</sub>/CH<sub>4</sub> (18%) > O<sub>2</sub>/N<sub>2</sub> (15%) > CO<sub>2</sub>/N<sub>2</sub> (5%). The permeability and selectivity were influenced by not only the thermal treatment temperature, but also the thermal treatment time, as shown in Table 1 and Table 2, the values varied with thermal treatment time at the annealing temperature of 330 °C. Both the thermal treatment temperature and the treatment time influence the cross-linking density, which might influence also the cross-linking sites shown in Scheme 2. The reason for the decline in selectivity with increased thermal treatment temperature is not yet clear. The decline in selectivity is presumably due to a change in the polymer structure during the decarboxylation and cross-linking process. For example, in Scheme 2, a phenyl radical could be involved in a cross-linking bond and create local packing disruptions, where the –COOH group was previously.

In most cases, cross-linking decreases the permeability of polymeric membranes,<sup>19</sup> especially for rubbery polymers, but this trend is not always seen for glassy polymers. Polyimides cross-linked with *p*-xylene diamine show a decreased gas permeability;<sup>22</sup> however, cross-linking of DABA-containing polyimides with diols leads to a more desirable increase in permeability for the dense film.<sup>10,15,16</sup> The above-described results show that the decarboxylation-induced thermal cross-linking also leads to an increase in gas permeability. Carbon dioxide, the most permeable gas in the cross-linked membranes followed by He and O<sub>2</sub>, and N<sub>2</sub> and CH<sub>4</sub>, shows the lower permeability increase. On the other hand, the lower permeability penetrants show the greatest increase with increasing heat treatment, thereby reducing selectivity with increased heat treatment temperature. A similar observation of an increased permeability and decreased selectivity with increased thermal treatment temperature was also observed in partially pyrolyzed 6FDA–ODA:DABA copolyimide membranes.<sup>33</sup>

Despite the small selectivity drop, the thermal cross-linked 6FDA–DAM:DABA membranes still showed good selectivity and exhibited much higher CO<sub>2</sub> and O<sub>2</sub> permeability compared to the un-cross-linked one. This trend can be beneficial for



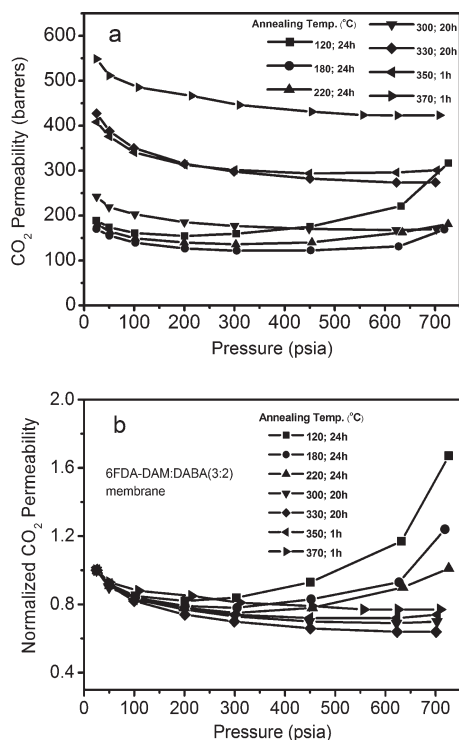


**Figure 6.** Fugacity corrected permeabilities (a), and normalized permeabilities (b) of CO<sub>2</sub> as a function of feed pressure under various annealing temperature.

CO<sub>2</sub>/CH<sub>4</sub>, CO<sub>2</sub>/N<sub>2</sub>, and O<sub>2</sub>/N<sub>2</sub> separations in many applications, but especially important is that the cross-linked membranes gained plasticization resistance for high CO<sub>2</sub> partial feed pressures.

#### Plasticization Resistance of the Cross-Linked Membranes.

Swelling-induced plasticization is a common phenomenon for polymer membranes in gas separation involving aggressive feed streams, such as CO<sub>2</sub> in natural gas. Plasticization occurs when a penetrant increases the mobility of polymer chain segments, thereby increasing the diffusion coefficients of all penetrants in the membrane. Plasticization causes an increase in permeability and a decrease in selectivity as the partial pressure of plasticizing penetrant such as CO<sub>2</sub> rises beyond a critical level. The plasticization pressure is defined as the pressure at which the permeability starts to increase with increasing pressure.<sup>2</sup> The permeabilities of 6FDA–DAM:DABA (3:2) membranes thermally treated under various temperatures were tested, and the pure gas CO<sub>2</sub> permeabilities are shown in Figure 6 as a function of the CO<sub>2</sub> upstream feed pressure. The curves can be grouped into two types according to the thermally treatment temperature relative to 300 °C. With thermally treatment temperature below 300 °C, the CO<sub>2</sub> permeabilities decreased with increasing of feed pressure up to a critical pressure, then an upturn in permeabilities were observed in Figure 6a. This is typical of the plasticization responses in glassy polymers. The plasticization response is more easily observed from the normalized permeability in Figure 6b where the CO<sub>2</sub> permeabilities were normalized with respect to the initial value measured at 25 psia. The plasticization pressure was 200–300 psia for the membrane annealed at 120 °C, 300–400 psia for the membrane annealed at 180 °C, and around 450 psia for the membrane annealed at 220 °C. The decreasing CO<sub>2</sub> permeability with increasing CO<sub>2</sub> pressure is consistent with the “dual mode sorption” and transport model predictions,

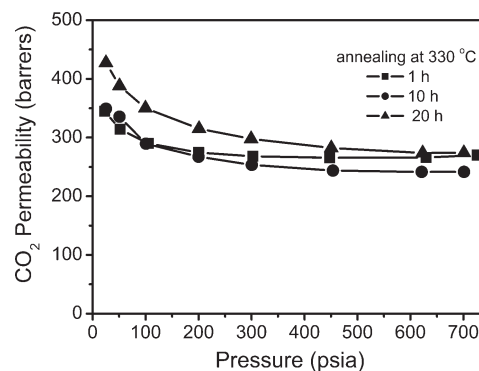


**Figure 7.** Fugacity corrected permeabilities of CO<sub>2</sub> as a function of feed pressure under various annealing time at 330 °C.

and this was valid until the plasticization of the polymer by CO<sub>2</sub> dominated. Part a and b of Figure 6 shows that for the membranes thermally treated above 300 °C, CO<sub>2</sub> permeabilities continued to decrease with increasing of feed pressure and did not show any signs of plasticization up to the highest CO<sub>2</sub> feed pressure of 700 psia tested in our work. For the 300 °C treated membrane, CO<sub>2</sub> permeability continued to decrease with increasing upstream pressure, characteristic of nonplasticized behavior. The strongly cross-linked membranes are stable when exposed to high CO<sub>2</sub> pressure continuously, whereas un-cross-linked membranes swell and are plasticized severely. For example, after being exposed to the highest CO<sub>2</sub> pressure of 700 psia for 20 h, the permeability of the membrane treated at 370 °C increased just 8%, while permeability of the membrane treated at 180 °C increased about 120%. These results are consistent with the thermal analysis results and solubility tests described above, and confirmed that the membrane annealed at 370 °C was cross-linked while at 180 °C it was not cross-linked. The cross-linked membranes reveal much higher permeability at the same feed pressure than the un-cross-linked ones, as can be seen in Figure 6a, the permeability of membranes show the same order as thermal treatment temperature of 370 °C > 350 °C, 330 °C > 300 °C > 220 °C > 180 °C. The lower permeabilities of membranes annealed at 220 and 180 °C versus that of 120 °C are due to the annealing effect prior to decarboxylation cross-linking, as discussed above. Figure 7 shows the effect of annealing time on CO<sub>2</sub> permeabilities for the membrane thermally treated at 330 °C. Treatment for 20 h produces strongly cross-linked membranes with high permeability and plasticization resistance. Treatment for 10 h, and even 1 h, still provides plasticization resistance; however, the trends vs feed pressure are different and distinguishable from experimental uncertainty. The higher CO<sub>2</sub> permeability at low CO<sub>2</sub> feed pressure for the 20 h heat treated samples were not anticipated. This behavior presumably reflects considerably greater unrelaxed excess volume trapped in the cross-linked glass, versus the less treated samples. Sorption studies of the so-called Langmuir capacities of these samples would be useful, but they are beyond the scope of this study, which focused on permeation properties.

**Effects of Cross-Linking on Mixed Gases Permeation Properties.** Permeation measurements were made with two mixtures of CO<sub>2</sub>/CH<sub>4</sub>, which mimic contaminated natural gas feed tested at 35 °C for total feed pressures up to 1000 psia, having a CO<sub>2</sub> content of 10.3% and 50.0%, respectively, both have an analytical uncertainty of ±2%, supplied by the vendors. A retentate flow was provided during these tests with the ratio of permeate/retentate

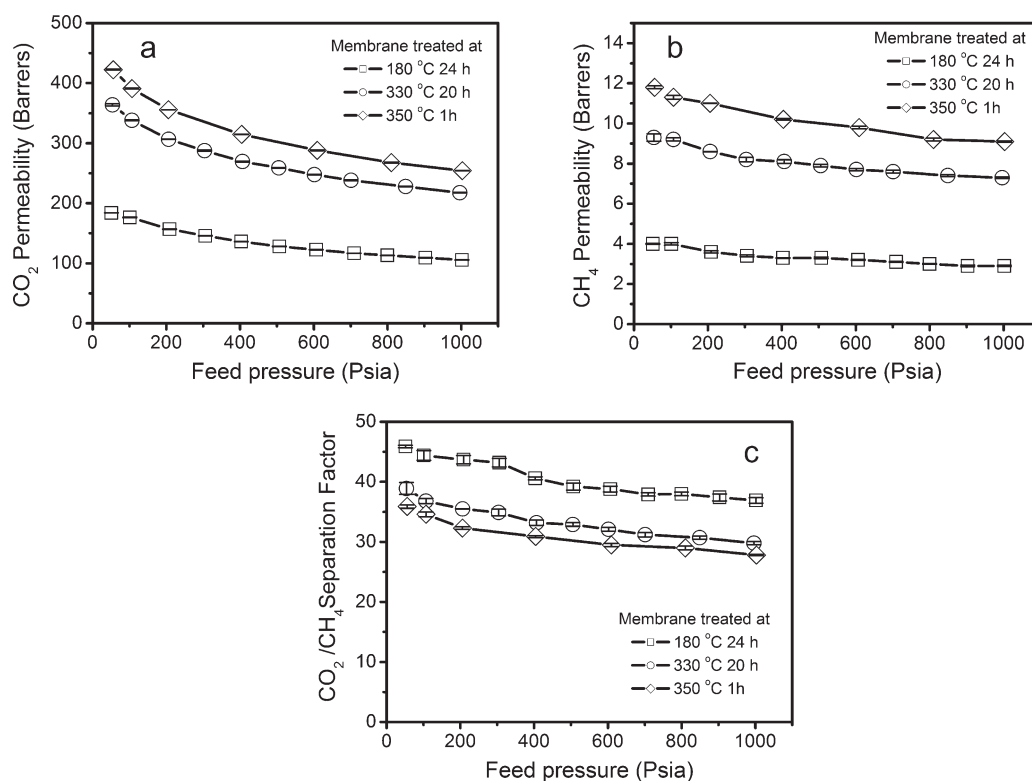


**Figure 8.** Mixed gas permeation using a 10/90 CO<sub>2</sub>/CH<sub>4</sub> at 35 °C: (a) CO<sub>2</sub> permeability, (b) CH<sub>4</sub> permeability, and (c) CO<sub>2</sub>/CH<sub>4</sub> separation factor.

flow less than 0.005, to maintain a constant transmembrane driving force along the membrane. For all the permeation experiments, the membrane was exposed to the feed for at least 2 h to allow sufficient equilibration time to reach steady state until the rate of pressure rise in the downstream receiver volume becomes constant. The measurement procedure is the same as for the pure gas test except the test was repeated 4–5 times. As the feed pressure increases, the components behave less ideally; therefore, the fugacity coefficients of CO<sub>2</sub> and CH<sub>4</sub> were used to calculate the permeability coefficients based on the partial fugacity deriving forces.

Figure 8 shows the permeation of the mixed gas of 10:90 CO<sub>2</sub>/CH<sub>4</sub> for typical membranes. It is seen from Figure 8a that the CO<sub>2</sub> permeability increases significantly with increasing thermal treatment temperature. The membrane cross-linked at 350 °C shows a CO<sub>2</sub> permeability about 2.5 times that of the un-cross-linked membrane annealed at 180 °C, and the CO<sub>2</sub> permeabilities decrease also slightly with the increasing of feed pressure until 1000 psia. Similar to CO<sub>2</sub>, Figure 8b shows that the CH<sub>4</sub> permeability also increases with the increasing thermal treatment temperature. The membrane cross-linked at 350 °C shows the CH<sub>4</sub> permeability rises to about 3 times that of the un-cross-linked membrane annealed at 180 °C, and the CH<sub>4</sub> permeabilities decrease slightly with increasing feed pressure. No plasticization response was observed even for the un-cross-linked membrane, which is presumably due to the low CO<sub>2</sub> partial pressure. Indeed, even at 1000 psia feed pressure, the CO<sub>2</sub> partial pressure is only 100 psia, which is much lower than the plasticization pressure observed in pure CO<sub>2</sub> permeation test. The CO<sub>2</sub>/CH<sub>4</sub> separation factor is higher than the ideal selectivity from pure gas permeation experiments, and the cross-linked membranes revealed lower separation factor than the un-cross-linked one. As shown in Figure 8c, the separation factor

decreases slightly at low pressures and finally reaches a plateau with increasing feed pressure. A similar decrease in both permeability (or permance) and CO<sub>2</sub>/CH<sub>4</sub> separation factor with increasing of feed pressure at low pressures was observed also in diol cross-linked 6FDA–DABA:DABA membranes.<sup>5,10,13,16,17,23</sup>

The permeation measurements for mixed gas of 50:50 CO<sub>2</sub>/CH<sub>4</sub> feed mixture were conducted to subject the membranes to a more aggressive condition. Figure 9 shows the permeation of the mixed gas of 50:50 CO<sub>2</sub>/CH<sub>4</sub> for typical membranes. Figure 9a shows that the cross-linked membrane has a much higher CO<sub>2</sub> permeability than the un-cross-linked one, which was annealed at 180 °C. The CO<sub>2</sub> permeability of cross-linked membrane decreased monotonically with the increasing of feed pressure. On the other hand, the un-cross-linked membrane shows an upturn in CO<sub>2</sub> permeability beyond the feed pressure of 500 psia, indicating that the membrane is plasticized. The plasticization in the un-cross-linked membrane is also indicated by the CH<sub>4</sub> permeability and CO<sub>2</sub>/CH<sub>4</sub> separation factor. As can be seen in Figure 9b, for the 50:50 CO<sub>2</sub>/CH<sub>4</sub> mixture the CH<sub>4</sub> permeability in the un-cross-linked membrane varies slightly initially but shows plasticization for feed pressures beyond 500 psia reflected by the upswing in CH<sub>4</sub> permeability and the drop in CO<sub>2</sub>/CH<sub>4</sub> separation factor (see Figure 9c). On the other hand, for the cross-linked membranes, CH<sub>4</sub> permeabilities decreased slightly at low pressure and remained unchanged at high pressure, with increasing feed pressure. Similar to CO<sub>2</sub>, CH<sub>4</sub> also has a higher permeability in the cross-linked membrane versus the un-cross-linked case, and the permeability increased with the increase of thermal treatment temperature. Figure 9c shows that the mixed gas CO<sub>2</sub>/CH<sub>4</sub> separation factor of cross-linked membrane decreases slightly with the increase of feed pressure and reached to a plateau while the un-cross-linked one revealed a marked drop. It is apparent that the un-cross-linked

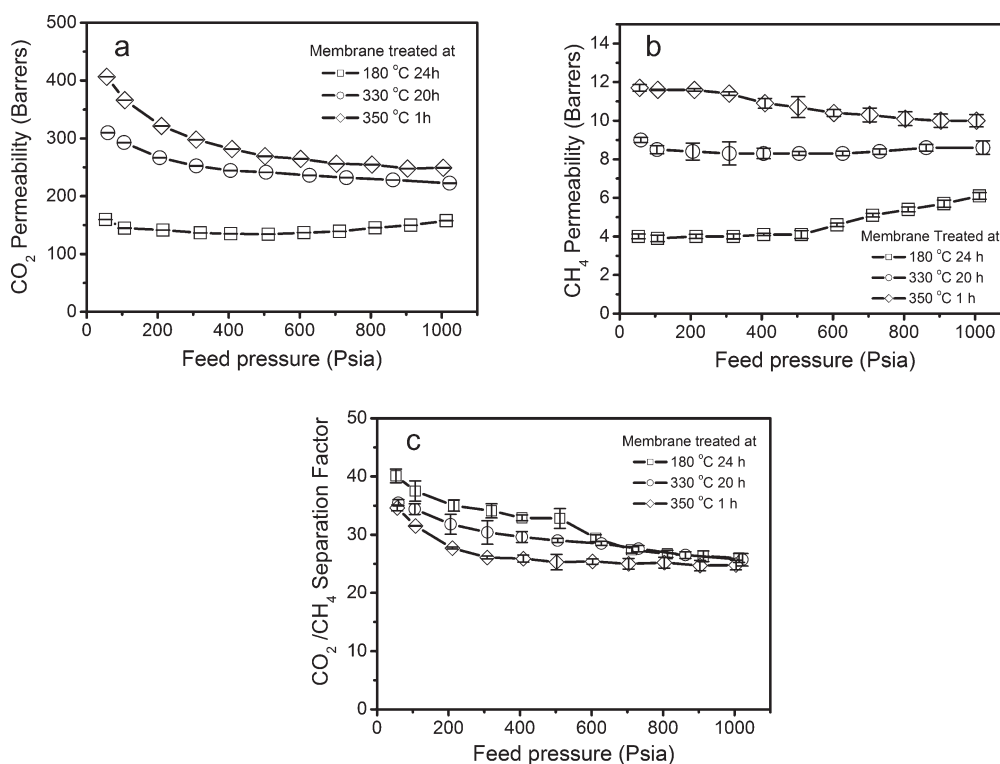


**Figure 9.** Mixed gas permeation using a 50/50 CO<sub>2</sub>/CH<sub>4</sub> at 35 °C: (a) CO<sub>2</sub> permeability, (b) CH<sub>4</sub> permeability, and (c) CO<sub>2</sub>/CH<sub>4</sub> separation factor.

membrane was swelled and/or plasticized in a 50/50 CO<sub>2</sub>/CH<sub>4</sub> mixture due to the higher CO<sub>2</sub> partial pressure, and the cross-linked membranes did not show such instability even up to the CO<sub>2</sub> partial pressure of 500 psia, or a feed pressure of 1000 psia.

On the basis of TG analysis and IR data described above, the removal of carboxylic acid groups, i.e., the formation of cross-linking, is complete for treatments at 330 °C for 20 h and 370 °C for 1 h; however, the permeation properties of both pure CO<sub>2</sub> and mixed gas are quite different for these treatments. The higher temperature leads to higher CO<sub>2</sub> permeabilities, without much decrease in CO<sub>2</sub>/CH<sub>4</sub> selectivity, suggesting that the transport properties may be optimized by cross-linking at higher temperatures, which is sufficient to quickly cross-link the polymer chains and open up the matrix without tightening the matrix through thermal annealing. This implies also that there might be two competing processes, cross-linking and annealing, which drive permeability in opposite directions. Lower temperature and longer annealing time might cause the polymer chains to become packed more densely and result in a reduction of gas permeability. Further research on this issue would be of interest; however, for ultimate application in hollow fibers with porous morphologies lower temperature annealing is desirable to prevent pore structure collapse.

The thick dense film works in this study provide insights about the material properties after various thermal treatments. The asymmetric structure of hollow fiber membranes adds complexity to membrane characterization. The detailed development and characterization of defect-free cross-linked hollow fiber membranes will be the primary focus of a subsequent paper. These preliminary results, however, show higher selectivity is achieved, and if modification of spinning or postspinning cross-linking treatment can minimize the support collapse, the attractive plasticization resistance seen with the dense films can be exploited more effectively.

## CONCLUSIONS

Decarboxylation-induced thermal cross-linking of 6FDA–DAM:DABA (3:2) polymeric membranes at temperatures much below the polymer glass transition temperature was achieved in dense films. Both the thermal treatment temperature and the thermal treatment time influence the extent of cross-linking. Membranes with significant cross-linking density can be achieved at temperatures as low as 330 °C for 20 h or 350 °C for 1 h. Cross-linking causes a markedly increase in permeability for all measured gases (He, O<sub>2</sub>, N<sub>2</sub>, CH<sub>4</sub>, and CO<sub>2</sub>) and a slight decrease in CO<sub>2</sub>/CH<sub>4</sub> selectivity. The selectivity of the cross-linked membrane can be maintained even under very aggressive CO<sub>2</sub> operating conditions that are not possible without cross-linking. Plasticization was observed at about 500 psia for an un-cross-linked membrane with a 50/50 CO<sub>2</sub>/CH<sub>4</sub> mixed gas. And plasticization resistance for cross-linked membrane was gained up to 700 psia for pure CO<sub>2</sub> gas or 1000 psia for 50/50 CO<sub>2</sub>/CH<sub>4</sub> mixed gas. Permeability of both CO<sub>2</sub> and CH<sub>4</sub> increased in cross-linked dense film membranes for either 10/90 or 50/50 CO<sub>2</sub>/CH<sub>4</sub> mixed gas, which is beneficial to CO<sub>2</sub>/CH<sub>4</sub> separation applications.

## AUTHOR INFORMATION

### Corresponding Author

\*Telephone: 1-404-385-2845. E-mail: wjk@chbe.gatech.edu.

## ACKNOWLEDGMENT

This research was supported by the U.S. Department of Energy Grant DE-FG02-04ER15510, and was supported in part by Award No. KUS-I1-011-21, made by King Abdullah University of Science and Technology (KAUST).

## REFERENCES

- (1) Baker, R. W.; Lokhandwala, K. *Ind. Eng. Chem. Res.* **2008**, 47 (7), 2109–2121.
- (2) Bos, A.; Punt, I. G. M.; Wessling, M.; Strathmann, H. *J. Membr. Sci.* **1999**, 155 (1), 67–78.
- (3) Datta, A. K.; Sen, P. K. *J. Membr. Sci.* **2006**, 283 (1–2), 291–300.
- (4) Lee, A. L.; Feldkirchner, H. L.; Stern, S. A.; Houde, A. Y.; Gamez, J. P.; Meyer, H. S. *Gas Sep. Purif.* **1995**, 9 (1), 35–43.
- (5) Wind, J. D.; Paul, D. R.; Koros, W. J. *J. Membr. Sci.* **2004**, 228 (2), 227–236.
- (6) Schell, W. J. *J. Membr. Sci.* **1985**, 22 (2–3), 217–224.
- (7) Bhide, B. D.; Voskericyan, A.; Stern, S. A. *J. Membr. Sci.* **1998**, 140 (1), 27–49.
- (8) Maya, E. M.; Lozano, A. E.; de Abajo, J.; De la Campa, J. G. *Polym. Degrad. Stab.* **2007**, 92 (12), 2294–2299.
- (9) Coleman, M. R.; Koros, W. J. *J. Membr. Sci.* **1990**, 50 (3), 285–297.
- (10) Hillock, A. M. W.; Koros, W. J. *Macromolecules* **2007**, 40 (3), 583–587.
- (11) Stern, S. A.; Mi, Y.; Yamamoto, H.; Stclair, A. K. *J. Polym. Sci., Part B: Polym. Phys.* **1989**, 27 (9), 1887–1909.
- (12) Kratochvil, A. M.; Koros, W. J. *Macromolecules* **2008**, 41 (21), 7920–7927.
- (13) Omole, I. C.; Miller, S. J.; Koros, W. J. *Macromolecules* **2008**, 41 (17), 6367–6375.
- (14) Staudt-Bickel, C. *Soft Mater.* **2003**, 1 (3), 277–293.
- (15) Staudt-Bickel, C.; Koros, W. J. *J. Membr. Sci.* **1999**, 155 (1), 145–154.
- (16) Wind, J. D.; Staudt-Bickel, C.; Paul, D. R.; Koros, W. J. *Ind. Eng. Chem. Res.* **2002**, 41 (24), 6139–6148.
- (17) Wind, J. D.; Staudt-Bickel, C.; Paul, D. R.; Koros, W. J. *Macromolecules* **2003**, 36 (6), 1882–1888.
- (18) Bos, A.; Punt, I. G. M.; Wessling, M.; Strathmann, H. *Sep. Purif. Technol.* **1998**, 14 (1–3), 27–39.
- (19) Bos, A.; Punt, I.; Strathmann, H.; Wessling, M. *AIChE J.* **2001**, 47 (5), 1088–1093.
- (20) Bos, A.; Punt, I. G. M.; Wessling, M.; Strathmann, H. *J. Polym. Sci., Part B: Polym. Phys.* **1998**, 36 (9), 1547–1556.
- (21) Kita, H.; Inada, T.; Tanaka, K.; Okamoto, K. *J. Membr. Sci.* **1994**, 87 (1–2), 139–147.
- (22) Liu, Y.; Wang, R.; Chung, T. S. *J. Membr. Sci.* **2001**, 189 (2), 231–239.
- (23) Omole, I. C.; Adams, R. T.; Miller, S. J.; Koros, W. J. *Ind. Eng. Chem. Res.* **2010**, 49 (10), 4887–4896.
- (24) McCaig, M. S.; Paul, D. R. *Polymer* **1999**, 40 (26), 7209–7225.
- (25) Hu, L.; Xu, X. L.; Coleman, M. R. *J. Appl. Polym. Sci.* **2007**, 103 (3), 1670–1680.
- (26) Chung, T. S.; Shao, L.; Tin, P. S. *Macromol. Rapid Commun.* **2006**, 27 (13), 998–1003.
- (27) Powell, C. E.; Duthie, X. J.; Kentish, S. E.; Qiao, G. G.; Stevens, G. W. *J. Membr. Sci.* **2007**, 291 (1–2), 199–209.
- (28) Cao, C.; Chung, T. S.; Liu, Y.; Wang, R.; Pramoda, K. P. *J. Membr. Sci.* **2003**, 216 (1–2), 257–268.
- (29) Prausnitz, J. M.; Lichtenthaler, R. N.; Azevedo, E. G. d., *Molecular thermodynamics of fluid-phase equilibria*, 3rd ed.; Prentice Hall: Upper Saddle River, NJ, 1999; p xxiii, 860 p.
- (30) *CRC handbook of chemistry and physics*; Chapman and Hall/CRCnetBASE: Boca Raton, FL, 1999.
- (31) Tanaka, K.; Kita, H.; Okano, M.; Okamoto, K. *Polymer* **1992**, 33 (3), 585–592.
- (32) Tanaka, K.; Okano, M.; Kita, H.; Okamoto, K.; Nishi, S. *Polym. J.* **1994**, 26 (10), 1186–1189.
- (33) Maya, E. M.; Tena, A.; de Abajo, J.; de la Campa, J. G.; Lozano, A. E. *J. Membr. Sci.* **2010**, 349 (1–2), 385–392.
- (34) Maya, E.; Lozano, A.; Deabajo, J.; Delacampa, J. *Polym. Degrad. Stab.* **2007**, 92 (12), 2294–2299.
- (35) Kim, Y. *J. Membr. Sci.* **2004**, 235 (1–2), 139–146.
- (36) Huang, R. Y. M.; Xiao, S.; Feng, X. S. *Polymer* **2007**, 48 (18), 5355–5368.
- (37) Park, H. B.; Han, S. H.; Jung, C. H.; Lee, Y. M.; Hill, A. J. *J. Membr. Sci.* **2010**, 359 (1–2), 11–24.
- (38) Huang, Y.; Paul, D. R. *Macromolecules* **2005**, 38 (24), 10148–10154.
- (39) Huang, Y.; Wang, X.; Paul, D. R. *J. Membr. Sci.* **2006**, 277 (1–2), 219–229.